nature portfolio

Peer Review File

Design of White Circularly Polarized Luminescence with High glum Across Entire Visible Regions by Dual-Loop Active Learning

Corresponding Author: Professor Gang Zou

This file contains all reviewer reports in order by version, followed by all author rebuttals in order by version.

Version 0:

Reviewer comments:

Reviewer #1

(Remarks to the Author)
Zou and coworkers reported a work focused on the dual-loop active learning framework integrating machine learning and large language models for the inverse design of high-performance white circularly polarized luminescence materials. The presented research simultaneously optimized multiple interdependent metrics (glum, CIE, FF and CRI) targeting a long-standing challenge in the field of WCPL and accelerating the discovery of materials with unprecedented chiral-photonic features. The combination of material chemistry (polymer fabrication), photochemistry (asymmetric emission), machine learning (WAE, TabPFN, Bayesian optimization) and device-engineering (CP-WOLEDs) makes this work interdisciplinary and very ambitious, reporting an exceptional WCPL-performance (a ternary system composed by PFO, F8BT and PFO-DBT macromolecules) in terms of glum (~1.77).
However…the authors have recently published an article (https://doi.org/10.1002/cjoc.70329) which reports the optical and chiroptical profiles (fluorescent spectra, CPL spectra, glum, etc.) of the same materials (PFO, F8BT and PFO-DBT films) exploiting the same chiral mechanism (twist-stacking design), fabricated on the same support ("The WCPL films with twisted-stacking (TS) structure were fabricated by overlaying a highly stretched PVA layer as a phase retarder onto above anisotropic fluorescent film, with a certain twisting angle of 45°" and "the CPL-active polyfluorenes films with twist-stacking structures were fabricated by overlaying a highly stretched PVA layer as a phase retarder onto above pre-prepared anisotropic fluorescent film, with a twist angle of ±45°") through the same methodology (spin-coating followed by thermal annealing treatment), and in both cases glum values are very similar (>1.5/~1.77). In the mentioned published paper, a pre-screening of the processing parameter (PVA thickness and stretching degree) was already carried out, hence the AI-assisted approach (performed in this submitted article) was a sort of refinement/optimization to obtain the white asymmetric emission from well-known ternary polyfluorene/PVA films. All this leads a remarkable conceptual overlap between the two articles, even if some novelties (the addition of rubrene and the implementation in the OLED chip prototype) were introduced.
I: Why have the authors used ChemDMF if they had already known (and published) the exceptional chiroptical properties of PFO, F8BT and PFO-DBT films?
II: As concerning the quaternary mixture, I couldn't find any explicit material composition (molar ratio or percentage composition) all along the manuscript neither in the supplementary information.
III: The authors justified the chirality transfer through a twist-stacking arrangement but no experimental evidence (for examples AFM, SEM, TEM ect.) was included.
IV: Rubrene was identified as the forth component, however "rubenene" was proposed by the the large language models (Figure S12).
V: In Figure S7, dark lines are almost chromatically indistinguishable (40/80μm, 50/100% and PFO/PFO-DBT). In part C, how is it possible that the PFO glum has a bisignate curve (~450/600nm) if the relative (monosignate) CPL maximum is located at ~430nm (Fig S9C, https://onlinelibrary.wiley.com/action/downloadSupplement?doi=10.1002/cjoc.70329&file=cjoc202501149-sup-0001-supinfo.pdf) ?
All this criticality do not allow the paper to match the criteria to publish on Nature Communications, therefore I cannot recommend it.

Reviewer #2

(Remarks to the Author)
The manuscript proposes a novel dual-loop active learning framework that integrates a large language model (ChemDMF), a Wasserstein autoencoder (WAE), Gaussian mixture model-Markov chain Monte Carlo (GMM-MCMC) sampling, TabPFN regression, and Bayesian optimization to accelerate the discovery of high-performance white circularly polarized luminescence (WCPL) materials. Starting from the PFO/F8BT/PFO-DBT ternary system, the authors optimize the color rendering index (CRI) and CIE coordinates in Loop I, and the asymmetry factor (glum) and spectral fill factor (FF) in Loop II. Through iterative optimization, a quaternary system incorporating a fourth component (Rub) achieves outstanding performance: CRI > 90, CIE (0.33, 0.33), |glum| ≈ 1.8, and FF ≈ 0.8. Circularly polarized white organic light-emitting diodes (CP-WOLEDs) are successfully fabricated, demonstrating the ability to tailor the correlated color temperature (CCT) on demand. Overall, this work is innovative and has potential research impact, but the following aspects require revision and supplementation.

(1) The formula (3) in the main text defines M = |glum| × (Ra / 100), and it is reported that “our proposed hybrid films exhibit both high |glum| of 1.8 and Ra of 90, leading to an exceptionally high M value up to about 1.62”. However, in SI Table S1, the same set of data is given as |glum|=1.77, Ra=90, and M=0.89, which deviates from the main text by a factor of two. Moreover, the M values in the table do not appear to be calculated according to the formula in the main text. Please unify the definition of M between the main text and the SI, recalculate all comparative data, and revise Figure 3e and Table S1 if necessary.

(2) In this work, an organic system with a glum as high as 1.8 was achieved, and the authors attribute this high glum to the optimized twisted-stacking structure. However, several control experiments may still be lacking, such as: (i) the glum of the emissive layer alone (without the PVA layer), (ii) the glum of the emissive layer combined with an unstretched PVA layer, and (iii) the glum of the emissive layer combined with a stretched PVA layer but with a twist angle of 0°. Without these baseline data, it is impossible to distinguish whether the high glum originates from the intrinsic chirality of the material, the linear polarization effect of PVA, or genuine circular polarization amplification arising from the twisted stacking. Therefore, it is recommended that at least above three types of control experiments be performed to improve the discussion of the high glum in this work.

(3) The specific numerical values of the 147 ternary data points and 26 Bayesian optimization samples used for training the model (including composition ratios, spectra, CRI, CIE coordinates, glum, FF, thickness, stretch ratio, etc.) are not provided in a table or data file format; they are only schematically shown in SI Figure S5. According to the journal's data availability policy, key data supporting the conclusions should be made publicly available or at least provided as supplementary material. Please compile all training and validation data into an Excel/CSV file and upload it as SI, or provide a link to a public data repository.

(4) In the Dual-loop active learning strategy design, the authors state that “the resulting WCPL performance is returned to Loop I as an additional constraint, guiding the next compositional search.” However, it is not specified in what form this return takes, whether the glum or FF is incorporated as part of the objective function to retrain the model in Loop I, or used as a screening threshold. The description in the text leans more toward a sequential execution: first, Loop I identifies the optimal composition, and then Loop II optimizes the structure for that fixed composition. Please provide additional details on the interaction mechanism of the dual loops to help readers understand how the two loops interact and form a closed loop.

(5) In the Iterative optimization of WCPL based on the ternary systems, it is stated that "The search space was bounded to 20 μm ≤ thickness ≤ 80 μm and 10% ≤ stretching degree ≤ 150%." This implies that thickness is treated as a continuous interval between 20 and 80 μm for running Gaussian process regression and acquisition function optimization. However, the Methods section shows that the actual available PVA film thicknesses are only three discrete values: 30 μm, 48 μm, and 80 μm, which introduces some ambiguity. It is necessary to clarify whether, if the optimization algorithm recommends a value such as 30.8 μm, the closest experimental thickness is chosen around the recommended value. Alternatively, the search space for Bayesian optimization should be redefined as the discrete set {30, 48, 80}, with the kernel function adjusted accordingly. If the authors actually achieved intermediate thicknesses by stacking multiple layers or multi-step stretching, this should also be explicitly stated.

Reviewer #3

(Remarks to the Author)
This manuscript reports an active learning including Bayesian optimization guided strategy for optimizing material compositions and processing parameters to obtain high-performance white circularly polarized films, and demonstrates a closed loop from model prediction to experimental validation. The topic is timely, and the overall workflow is potentially valuable for data-driven materials optimization. However, several important issues remain insufficiently addressed.
1.Please provide more justification for the use of a WAE latent space in Loop I. Considering ternary or quaternary compositional systems, the intrinsic dimensionality remains limited under simplex constraints, and it is therefore not yet clear that latent space modeling is necessary. The authors should clarify the advantage WAE provides over operating directly in the original composition space.
2.The proposed framework may be overengineered for the limited dataset (e.g. 272 samples for WAE and 26 for BO). Under such small data conditions, complex models may be unstable and difficult to validate rigorously. Therefore, stronger evidence is needed to justify the methodology, for example through learning curves, repeated cross-validation, etc.
3.The description of Loop II needs further clarification. The manuscript indicates that Bayesian optimization was performed with a GP surrogate, while several other regressors (including TabPFN) were benchmarked separately. The authors should clarify the role of these models and explain why GP, rather than the best-performing regressor, was used in the BO loop.

4.A structure comprising a commercial UV LED chip externally coupled to emissive films is an optically photoluminescence-based color conversion device, not an OLED or CP-WOLED. The use of “electroluminescence” and “CP-WOLED” should be revised.
5.The current data do not seem sufficient to justify stronger statements such as “direct deployment” in illumination or full-color 3D display applications. For a UV-LED-excited conversion device, application relevance should be supported by additional metrics such as photostability under continuous UV irradiation, operational lifetime, color stability over time, conversion efficiency or luminous efficacy, etc.
6.The conclusion may be somewhat overgeneralized. The present work demonstrates a promising proof-of-concept in a specific system, but the broader claim of “great fundamental value” for the accelerated discovery of novel optically functional materials and devices appears stronger than what is directly supported by the current results. A more cautious and specific conclusion would be more appropriate.
7.The current data availability statement is inadequate for a data-driven study, as the dataset is central to the main claims and necessary for reproducibility. The authors should publicly release the data required to reproduce the main results, or clearly justify any restrictions.
8.The claimed superiority over literature is not fully convincing without comparable measurement conditions, especially since CPL-related metrics such as g values are highly sensitive to calibration and testing procedures. Stronger validation of the key metrics is therefore needed, including reproducibility, uncertainty estimates, and preferably independent verification.

Version 1:

Reviewer comments:

Reviewer #1

(Remarks to the Author)
The authors of the present manuscript (NCOMMS-26-027357A) took a good wealth of time to respond to the reviewers’ comments and questions, explaining their point of view in good detail in the responses to the reviewers and transferring a few of the explained changes in the text (and SI). In my opinion, points 2-5 were carefully addressed, but point 1 (the key-one) is not clarified yet.
At this point, I would like to make some more comments: considering a chronological timeline, authors affirmed that “The published article (https://doi.org/10.1002/cjoc.70329) was a subsequent empirical validation inspired by the preliminary material screening of this overarching project” and that “the material systems adopted in both studies were initially screened and recommended by ChemDFM, an in-house, chemistry-oriented large language model proposed in this work”, but in the published article authors wrote that a biomimetic approach (mentioning also the Chrysina gloriosa) was adopted and no chemistry-oriented large language model (ChemDFM) was cited in their biomimetic design strategy for polyfluorenes selection. How is it possible? Again, if the published articles was an experimental characterization and performance validation, why did not authors cite it in the bibliography of the current submitted manuscript? The published article was accepted on 25 September 2025 (much earlier than the present submission). Coherently with my first revision, I still think that the present article has a remarkable conceptual overlap with the published work, even if some novelties (already discussed) were introduced. As stated by the authors “The present work achieves a systematic optimization of compositional and processing parameters “. At this point, I think that editor should decide if an AI-driven implementation for a forth component (rubrene) and a WCPL device prototype are a valid advancement (compared to the published article) which deserves a publication on Nature Communication.

Reviewer #2

(Remarks to the Author)
The authors have answered all questions, and I suggest to accept in present version.

Reviewer #3

(Remarks to the Author)
The authors have addressed the concerns I previously raised, and I am pleased to see a significant improvement in the scientific rigor and overall quality of the paper. I do not have any further questions or issues to raise.

中国科学技术大学
University of Science and Technology of China

Prof. Gang Zou
Department of Polymer Science and Engineering
University of Science and Technology of China
Jinzhai Road 96#, Baohe District, Hefei 230026 China
Email: gangzou@ustc.edu.cn

July 9, 2026

Dear Editor，

Thank you very much for your e-mail dated on 21-April-2026 regarding the revision on the above manuscript (NCOMMS-26-027357). We appreciate the valuable time and professional feedback provided by the reviewers, which are very helpful to improve the quality of the paper.

Regarding the editor's concern about the novelty of this work compared with previously published literatures [10.1002/cjoc.70329; 10.1038/s41467-025-60310-6], we systematically compared our work with existing studies and comprehensively clarified the unique advances and core innovations of the present work, with a comparative summary table newly supplemented in the revised manuscript for intuitive illustration.

Most previous circularly polarized luminescence (CPL) studies via twisted-stacking strategy from our group (including 10.1002/cjoc.70329) and other peers merely utilize single luminescent components to fabricate monochromatic chiral films. For multicolor emission, conventional approaches physically isolate distinct luminophores into discrete layers to avoid the Förster resonance energy transfer (FRET) interference. In stark contrast, this work achieves broadband white circularly polarized luminescence (WCPL) via multicomponent conjugated polymer blending within a single emissive layer. Intermolecular FRET between mixed components invalidates simple linear superposition of individual single-component spectra, while coupled compositional ratios and stacking fabrication parameters together form an ultrahigh-dimensional parameter space (up to 10^9). Such a complex system cannot be efficiently optimized by conventional trial-and-error experimentation or vanilla machine learning pipelines.

Our previous transfer learning framework (10.1038/s41467-025-60310-6) was exclusively designed for monochromatic emitters and only optimized stacking parameters. Directly migrating this single-loop model to our multicomponent white-light system leads to severe prediction bias, which originates from mismatched input spectral features, incompatible multi-objective constraints, and drastically different parameter dimensionality between monochromatic and white-light systems. Moreover, WCPL performance metrics (g_{lum}, CRI, *FF*, CIE chromaticity coordinates) are mutually coupled: enhancing one figure of merit inevitably trades off others, mandating simultaneous multi-objective balancing.

To tackle this bottleneck, we propose an innovative dual-coupled loop active learning framework that realizes multi-objective optimization targeting high CRI, ideal white-light CIE coordinates, high g_{lum} across the full visible spectrum and high *FF*, using only ~200 experimental datasets. Loop I (component optimization): Combines Wasserstein Autoencoder (WAE) and GMM-MCMC sampling to tune multicomponent blending ratios, prioritizing white-light chromatic quality (CRI and CIE coordinates). Loop II (process optimization): Leverages Gaussian process Bayesian optimization with composite acquisition functions to independently adjust the thickness and stretching strain of PVA phase retardation layers, optimizing high g_{lum} across the full visible spectrum.

Earlier landmark active learning paradigms, such as the single-loop alloy screening workflow reported by Rao et al. (Science, 2022, 378, 78–85), only adopt a single-loop architecture optimized for the Invar alloys combination of low thermal expansion coefficient and high configurational entropy. Differing fundamentally from all single-loop counterparts, our work establishes a generative dual-loop active learning pipeline with bidirectional closed-loop feedback between two physically decoupled yet mutually dependent optimization modules. This design enables dynamic synergistic balancing between white-light chromatic performance and chiroptical performance.

As summarized in the newly added comparative table in the revised manuscript, existing representative works only adopt single-loop machine learning workflows for either single-component monochromatic CPL or single-property alloy exploration, whereas our study is the first to deploy a dual-coupled loop active learning strategy for multi-component WCPL multi-objective optimization. This structural design that separates composition and process optimization based on distinct physical mechanisms constitutes the core novelty of this work, which is thoroughly elaborated in the revised *Introduction* section.

	CJC, 2025, DOI:10.1002/cjoc.70329	Nat. Commun., 2025, DOI:10.1038/s41467-025-60310-6	Our work	Science, 2022, DOI:10.1126/science.abo4940
Optimization Target	1.Single-band CPL 2.High luminescence dissymmetry factor(g_{lum})	1.Single-band high circularly polarized phosphorescence (CPP) g_{lum} 2.Narrow FWHM	1.High CRI and ideal CIE coordinate 2. High g_{lum} across the full visible spectrum	1.Low thermal expansion coefficient 2. High configurational entropy
Material System	Single-component CPL film	Single-component CPP film	Multi-component WCPL film	High-entropy Invar alloys
Core Innovations	CPL for encryption	Transfer learning for monochromatic CPP	Dual-loop active learning for multi-objective optimization with a small dataset	Single-loop active learning for alloy screening
ML Modules	/	Single-loop transfer learning	Dual coupled loops active learning	Single-loop active learning
Emission range	Single-band	Single narrow band	/	Full visible spectrum

In addition, we have addressed all the concerns of the reviewers with additional experiments and discussions. Accordingly, we have meticulously revised our manuscript and supporting materials with the corresponding parts highlighted and resubmitted our revised version. The details of the point-by-point response are given on the following pages.

We hope the present manuscript have been promoted greatly and now it could satisfy the quality required by your esteemed journal. Thank you very much again for your efforts in this regard, and we look forward to hearing from you soon.

Sincerely

Gang Zou

Reviewer 1:
Comments to the Author

Zou and coworkers reported a work focused on the dual-loop active learning framework integrating machine learning and large language models for the inverse design of high-performance white circularly polarized luminescence materials. The presented research simultaneously optimized multiple interdependent metrics (g_{lum}, CIE, *FF* and CRI) targeting a long-standing challenge in the field of WCPL and accelerating the discovery of materials with unprecedented chiral-photonic features. The combination of material chemistry (polymer fabrication), photochemistry (asymmetric emission), machine learning (WAE, TabPFN, Bayesian optimization) and device-engineering (CP-WOLEDs) makes this work interdisciplinary and very ambitious, reporting an exceptional WCPL-performance (a ternary system composed by PFO, F8BT and PFO-DBT macromolecules) in terms of g_{lum} (~1.77).
However the authors have recently published an article (https://doi.org/10.1002/cjoc.70329) which reports the optical and chiroptical profiles (fluorescent spectra, CPL spectra, g_{lum}, etc.) of the same materials (PFO, F8BT and PFO-DBT films) exploiting the same chiral mechanism (twist-stacking design), fabricated on the same support ("The WCPL films with twisted-stacking (TS) structure were fabricated by overlaying a highly stretched PVA layer as a phase retarder onto above anisotropic fluorescent film, with a certain twisting angle of ±45° " and "the CPL-active polyfluorenes films with twist-stacking structures were fabricated by overlaying a highly stretched PVA layer as a phase retarder onto above pre-prepared anisotropic fluorescent film, with a twist angle of ±45 ° ") through the same methodology (spin-coating followed by thermal annealing treatment), and in both cases g_{lum} values are very similar (>1.5/~1.77). In the mentioned published paper, a pre-screening of the processing parameter (PVA thickness and stretching degree) was already carried out, hence the AI-assisted approach (performed in this submitted article) was a sort of refinement/optimization to obtain the white asymmetric emission from well-known ternary polyfluorene/PVA films. All this leads a remarkable conceptual overlap between the two articles, even if some novelties (the addition of rubrene and the implementation in the OLED chip prototype) were introduced.

1. Why have the authors used ChemDFM if they had already known (and published) the exceptional chiroptical properties of PFO, F8BT and PFO-DBT films?
Reply:
We highly appreciate the reviewer's careful comparison and insightful comments. We would like to clarify the logical correlation, research timeline and innovative positioning of the two studies to address the concern of conceptual overlap.

The research prensented in this manuscript was was conducted primarily as a comprehensive methodological study. The published article (https://doi.org/10.1002/cjoc.70329) was a subsequent empirical validation inspired by the preliminary material screening of this overarching project. Due to distinct journal

review cycles, the relevant experimental results were published ahead of schedule, while this manuscript has undergone long-term submission and repeated revisions.

Notably, the material systems adopted in both studies were initially screened and recommended by ChemDFM, an in-house, chemistry-oriented large language model proposed in this work. The published study merely focused on experimental characterization and performance validation, yet it did not involve AI-driven parameter design or multi-objective optimization that forms the core of this manuscript. The present work achieves a systematicoptimization of compositional and processing parameters, extends the research scope to a quaternary blending system, and further demostrates a UV-LED coupled WCPL device prototype. These original contributions clearly differentiate this manuscript from the prior publication and strongly highlight the novelty and uniqueness of our AI-assisted design strategy.

2. As concerning the quaternary mixture, I couldn’t find any explicit material composition (molar ratio or percentage composition) all along the manuscript neither in the supplementary information.

Reply:

We apologize for the inadequate description for the quaternary mixture composition in the initial submission, which has led to reading confusion.

In the revised manuscript, we have supplemented the detailed volume ratios of all multicomponent systems within the **Methods** section and the **Supporting Information**. The proportional parameters of each component in the blending systems are now clearly specified, rendering the material formulas are fully explicit and experimentally repeatable. We sincerely thank the reviewer for pointing out this omission.

We have added the discussion on **Methods**, according to the reviewer’s helpful suggestions, as shown below:

“For the blended WCPL films, functional components were separately prepared as stock solutions with identical initial concentrations. All blended films were subsequently fabricated by mixing these homogeneous stock solutions according to fixed volume ratios of each component. Throughout the sample preparation, only the volume ratio of each stock solution was adjusted to guarantee reliable experimental control and good batch-to-batch consistency. The complete formulation parameters for both ternary and quaternary systems have been supplemented in Table S2 and S3 of the Supporting Information to facilitate result interpretation and experimental reproducibility.”

Table S2. The composition and performance of the samples for ternary systems that were tested during the optimization process. The formulations are ranked from best to worst according to their performance in the optimization experiments.

Formulation			Performance			
PFO	F8BT	PFO-DBT	CIE x	CIE y	CCT	Ra
80	0.3	7	0.36	0.35	4528	87
80	0.5	10	0.37	0.36	4262	88
90.4	0.7	9.6	0.37	0.35	4124	84
90.3	1	9.7	0.37	0.38	4209	89
89.9	1	10.1	0.38	0.38	4085	89
80	0.5	7	0.35	0.39	4977	88
92.7	0.8	7.3	0.36	0.39	4595	90
91.1	0.8	8.9	0.38	0.39	4196	90
12	0.3	3	0.38	0.36	3759	82
91.9	1	8.1	0.37	0.40	4424	91
92.3	1	7.7	0.37	0.40	4561	89
87.9	0.3	12.1	0.36	0.31	4111	71
18	0.3	5	0.41	0.36	3216	87
18	0.3	7	0.40	0.35	3135	82
15	0.3	7	0.41	0.35	2896	82
12	0.3	5	0.39	0.32	3205	69
18	0.3	9	0.40	0.31	2894	72
88.6	0.5	11.4	0.37	0.30	3377	65
15	0.6	9	0.42	0.35	2845	79
15	0.6	7	0.42	0.37	2932	84
12	0.3	1	0.38	0.42	4338	85
15	0.3	9	0.41	0.32	2726	72
18	0.9	3	0.41	0.41	3587	87
3	0.9	9	0.39	0.30	2763	69
6	0.3	3	0.40	0.34	3151	67
48	1	10	0.42	0.41	3405	86

15	0.9	5	0.43	0.40	3081	86
18	0.3	1	0.37	0.43	4498	80
15	0.9	7	0.42	0.37	2930	78
12	0.6	3	0.43	0.40	3110	85
18	0.6	3	0.43	0.40	3090	85
18	0.6	9	0.44	0.36	2616	82
18	1.2	5	0.42	0.39	3170	80
18	0.6	7	0.44	0.36	2655	81
18	0.9	5	0.41	0.38	3187	75
18	1.2	7	0.42	0.38	3042	75
15	0.9	9	0.43	0.36	2742	76
9	0.3	3	0.44	0.37	2740	79
12	0.3	9	0.39	0.30	2824	61
78.2	3	18.9	0.42	0.42	3385	85
12	0.6	9	0.41	0.32	2768	63
15	1.5	9	0.44	0.38	2826	80
38.1	1.2	10.7	0.43	0.39	2948	78
12	0.6	5	0.42	0.36	2988	66
12	0.9	7	0.43	0.36	2798	71
18	1.2	9	0.42	0.36	2861	69
3	0.9	5	0.46	0.38	2516	87
12	0.3	7	0.42	0.32	2510	66
75.1	3.2	21.1	0.43	0.41	3103	81
12	0.9	9	0.43	0.35	2655	70
87	1.9	11.1	0.40	0.45	3955	86
12	1.2	9	0.42	0.35	2889	65
15	1.5	7	0.45	0.41	2888	85
3	1.2	9	0.43	0.32	2319	69
3	0.9	7	0.45	0.36	2361	80
12	0.6	7	0.44	0.35	2520	72
3	0.3	1	0.45	0.42	3010	88
18	1.5	3	0.43	0.44	3409	87

18	1.5	5	0.43	0.39	2972	76
3	0.3	3	0.44	0.36	2608	72
12	0.9	5	0.44	0.39	2751	77
18	0.9	9	0.42	0.34	2679	62
6	0.3	5	0.41	0.31	2672	57
6	0.9	5	0.42	0.36	2907	65
15	0.3	1	0.38	0.45	4413	78
9	0.3	5	0.44	0.34	2405	68
6	0.6	1	0.43	0.45	3526	87
15	1.2	3	0.42	0.45	3570	87
6	0.6	3	0.44	0.39	2858	75
12	1.2	5	0.45	0.40	2727	80
62.1	2.5	35.4	0.43	0.35	2613	65
12	1.2	7	0.45	0.38	2603	76
3	1.2	7	0.47	0.38	2385	82
3	0.6	3	0.45	0.38	2658	75
9	0.3	7	0.44	0.33	2244	67
18	1.5	7	0.44	0.38	2757	70
9	0.9	3	0.45	0.40	2743	78
9	0.6	3	0.46	0.40	2557	81
18	1.5	9	0.44	0.38	2671	69
3	0.6	1	0.45	0.45	3165	87
18	0.9	7	0.44	0.36	2569	64
3	1.2	5	0.48	0.40	2410	86
6	0.6	5	0.43	0.34	2511	59
3	0.3	5	0.42	0.30	2371	54
12	0.6	1	0.41	0.46	3837	82
9	0.6	5	0.46	0.38	2413	73
3	0.6	5	0.45	0.36	2344	68
6	0.9	1	0.44	0.46	3290	86
12	1.5	5	0.46	0.40	2638	73
12	1.5	3	0.46	0.43	2864	81

9	0.9	5	0.46	0.38	2496	71
9	0.9	1	0.44	0.47	3381	87
9	0.3	9	0.44	0.31	2080	60
9	1.2	9	0.42	0.33	2525	52
12	1.5	7	0.46	0.38	2480	68
6	1.2	3	0.47	0.42	2644	81
12	0.9	1	0.41	0.48	3907	81
6	0.6	7	0.43	0.31	2333	51
9	1.2	3	0.47	0.41	2592	77
9	1.2	1	0.45	0.47	3343	86
9	1.5	3	0.47	0.43	2745	79
6	1.2	5	0.47	0.38	2331	70
9	0.9	9	0.45	0.33	2150	59
18	0.6	1	0.40	0.48	4157	75
18	0.9	1	0.39	0.48	4339	75
18	1.2	1	0.39	0.48	4348	75
6	0.9	7	0.44	0.33	2238	54
3	0.3	7	0.44	0.30	2039	53
12	1.5	1	0.43	0.48	3622	83
15	0.6	1	0.39	0.48	4313	73
15	0.9	1	0.40	0.48	4108	76
3	0.6	7	0.47	0.34	2064	63
6	1.2	1	0.47	0.46	2869	87
9	1.5	5	0.47	0.39	2497	68
9	1.5	1	0.44	0.48	3546	84
3	0.9	1	0.47	0.47	3019	87
12	1.2	1	0.43	0.48	3737	80
9	0.6	7	0.48	0.35	2000	66
9	0.6	9	0.46	0.32	1978	58
6	0.9	3	0.47	0.40	2481	68
6	1.5	1	0.47	0.47	2899	87
9	1.2	5	0.48	0.39	2284	70

6	0.3	7	0.38	0.26	2669	38
3	0.3	9	0.45	0.30	1952	53
6	1.2	9	0.46	0.34	2066	58
12	1.5	9	0.46	0.36	2235	59
9	1.5	7	0.47	0.37	2290	62
6	1.5	3	0.49	0.42	2335	78
6	0.9	9	0.43	0.30	2120	45
6	1.5	7	0.49	0.37	2089	66
3	1.5	1	0.50	0.45	2547	84
18	1.5	1	0.40	0.50	4161	74
9	0.9	7	0.48	0.36	2049	61
6	1.2	7	0.48	0.35	2024	61
3	1.5	5	0.49	0.37	2050	63
9	1.2	7	0.48	0.36	2047	61
15	1.5	1	0.40	0.50	4160	72
6	1.5	5	0.50	0.38	2053	69
15	1.2	1	0.41	0.50	4006	73
6	1.5	9	0.48	0.34	1918	58
3	1.5	3	0.50	0.40	2158	71
9	1.5	9	0.47	0.34	2007	54
3	1.5	9	0.42	0.27	1966	39
6	0.6	9	0.41	0.26	2016	31
3	1.5	7	0.51	0.36	1775	60
6	0.3	9	0.39	0.24	2158	25
3	0.6	9	0.35	0.22	2889	25

Note: All values in the formulation are given as relative volume parts, defining the volume ratio of each component in the blend.

Table S3. The composition and performance of the samples for quaternary systems that were tested during the optimization process. The formulations are ranked from best to worst according to their performance in the optimization experiments.

Formulation				Performance			
PFO	F8BT	PFO-DBT	RUB	CIE x	CIE y	CCT	Ra
85	0.5	10	8	0.33	0.33	5720	90
85	0.5	12	10	0.33	0.33	5482	84
75	0.5	10	5	0.35	0.36	4938	91
80	0.5	12	8	0.35	0.34	4696	86
82	0.5	15	10	0.34	0.33	5017	82
82.4	0.5	12.2	5.4	0.35	0.35	4830	86
70	0.5	14	10	0.35	0.34	4773	84
72	0.5	12	8	0.35	0.34	4733	85
80	0.5	15	10	0.35	0.34	4692	85
82	0.5	10	10	0.34	0.37	5280	89
80	0.5	10	8	0.36	0.36	4580	89
20	0.3	2	1	0.36	0.38	4682	91
20	0.5	2	2	0.35	0.38	4860	89
75	0.5	15	10	0.36	0.35	4304	82
18	0.3	3	2	0.35	0.32	4648	75
21	0.3	2	2	0.35	0.38	5002	88
83.8	0.5	12.5	3.7	0.35	0.32	4474	75
42	1	10	2	0.36	0.38	4485	90
70	0.5	16	10	0.36	0.33	4241	77
20	0.3	4	2	0.33	0.30	5368	74
70	0.5	16	16	0.37	0.37	4131	86
12	0.3	3	2	0.34	0.31	5021	70
80	0.5	18	10	0.36	0.32	4200	75
65	0.5	15	10	0.38	0.36	3989	82
86.5	0.5	6.3	7.2	0.33	0.39	5505	83
37	1	8.8	4.1	0.39	0.37	3806	87

37	1	8.4	3.8	0.39	0.38	3835	88
18	0.3	2	7	0.33	0.39	5663	80
18	0.3	3	5	0.38	0.33	3595	78
31	1	10	16	0.38	0.39	4255	89
23	0.5	2	2	0.40	0.38	3514	90
25	0.5	2	2	0.35	0.40	5037	84
36	1	11	1.9	0.39	0.36	3605	82
73.1	0.5	17.9	9	0.37	0.32	3894	69
25	0.2	1	1	0.34	0.39	5391	78
18	0.3	3	3	0.32	0.29	6547	69
25.6	1.8	13.6	8.9	0.40	0.38	3475	88
38	1	4.6	4.9	0.38	0.41	4189	89
37	1	3.7	8.4	0.37	0.40	4555	84
12	0.3	3	5	0.39	0.33	3392	74
70	0.5	14	8	0.40	0.36	3446	78
12	0.3	3	3	0.34	0.30	5143	63
37	1	4.4	7.4	0.38	0.41	4208	87
40	1	3.7	4.9	0.37	0.41	4411	85
40	1	7.7	1.9	0.37	0.42	4574	85
38	1	4.2	7.4	0.38	0.42	4301	86
14.7	1	19.8	14.6	0.40	0.33	2977	74
42	1	4.5	2.6	0.39	0.42	4150	88
25	0.3	1	1	0.33	0.41	5737	72
27	1.5	8	10	0.42	0.40	3385	88
26.3	2.3	18.8	2.5	0.42	0.38	3053	84
20	1	2	2	0.39	0.43	4119	87
23	0.5	1.5	2	0.36	0.43	4745	80
37	1	2.7	9.4	0.37	0.43	4599	80
26.2	2	10.3	11.4	0.42	0.41	3448	87
32	1	6	10	0.37	0.43	4569	80
83	0.5	5.9	11.1	0.34	0.43	5244	74
40	1.3	3.7	4.9	0.38	0.44	4327	82

14.3	1.3	8	30	0.42	0.43	3541	88
20	0.3	1	1.5	0.33	0.42	5554	70
38	1	5	5	0.37	0.44	4519	80
33	1	3.5	12.8	0.38	0.44	4382	81
17.5	2.8	13.3	16.3	0.44	0.41	2967	88
12.4	1.6	8	33	0.44	0.42	3012	91
12	0.4	2	7	0.40	0.44	4020	85
32	1	5.6	11.2	0.38	0.44	4488	78
17.5	2.5	13.3	16.3	0.44	0.40	2860	81
20	0.5	1	1	0.35	0.44	4984	73
25.5	2.5	17.4	4.6	0.45	0.39	2654	81
17.5	2.5	7	16	0.44	0.45	3258	88
38	1	4.6	6.8	0.36	0.45	4838	73
30	1	3.2	16.5	0.35	0.45	5210	66
20.8	6	20.9	2.2	0.47	0.41	2525	82
23.3	7.3	14.3	5.1	0.48	0.43	2567	85
9.4	7.8	18.7	14.1	0.49	0.40	2292	77
15.5	9.2	18.8	6.5	0.49	0.42	2369	80
12.4	1.6	2	33.8	0.39	0.47	4235	62
12.4	1.6	2.2	33.8	0.55	0.40	1722	90
14.1	15.2	13.7	7	0.50	0.41	2199	73
12.6	11	3.5	22.9	0.52	0.45	2268	85
10.6	3.2	18.6	17.6	0.53	0.36	1690	74
16.7	16.3	14.1	3	0.51	0.42	2220	75
7	14.2	10.8	18	0.52	0.39	1895	71
10.7	1.3	18.9	19.1	0.55	0.35	1480	75
15.2	2.3	7.1	25.4	0.57	0.36	1407	81
7.2	16.6	10.9	15.3	0.54	0.40	1841	68
5.6	10.1	17.3	16.9	0.55	0.38	1617	73
14.3	1.3	1	34	0.38	0.52	4574	54
8	14.3	23.3	4.4	0.53	0.36	1622	55
10.4	3.2	16.4	19.9	0.59	0.35	1248	79

3.8	9.6	28.6	7.9	0.54	0.35	1534	49
2	12	24.2	11.8	0.55	0.35	1482	50

Note: All values in the formulation are given as relative volume parts, defining the volume ratio of each component in the blend.

3. The authors justified the chirality transfer through a twist-stacking arrangement but no experimental evidence (for examples AFM, SEM, TEM ect.) was included.

Reply:

We sincerely appreciate the reviewer's valuable suggestion regarding the experimental validation of the chirality induction mechanism.

In this work, the observed circularly polarized luminescence (CPL) arises from macroscopic structural chirality constructed via the twist-stacking configuration, rather than inherent molecular chirality. The rational integration of linearly polarized luminescent layers and phase retardation layers with a centain twisted stacking angle enables efficient conversion from linearly polarized emission into circularly polarized luminescence, and the related mechanism has been demonstrated in the referenced literature (Adv. Mater. 2023, 35, 2209539).

To provide direct and convincing structural evidence, we have supplemented AFM, cross-sectional SEM, and polarizing microscope（POM） characterizations of the emissive layer to systematically reveal its surface morphology, layered thickness, uniform orientation, and polarization-dependent optical performance. These results clearly verified the excellent uniformity, desirable anisotropy, and robust polarized luminescence characteristics of the emissive layer within the well-defined twist-stacking architecture, which contributes significantly to the emergence of CPL .

The corresponding characterization results and detailed discussions have been incorporated into the revised manuscript (page 7, paragraph 2) and **Supporting Information** according to the reviewer's helpful suggestions, as follows.

"The surface morphology of the hybrid film was observed by atomic force microscopy (AFM), revealing that the annealed film was very smooth with a relatively low average roughness (Supplementary Fig. 7). Scanning electron microscope (SEM) cross-section characterizations indicated that the thickness of the film was about 30 nm (Supplementary Fig. 8). The polarization microscope images verified the anisotropic orientation of hybrid film (Supplementary Fig. 9)."

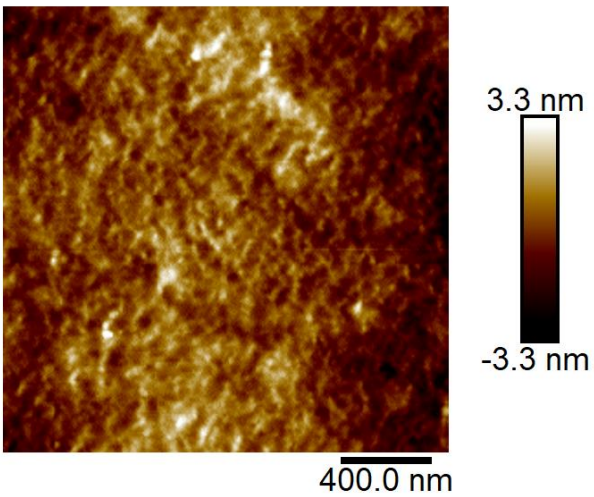

Figure S7. AFM images of the surface morphology of the emissive layer in the twisted-stacking hybrid film.

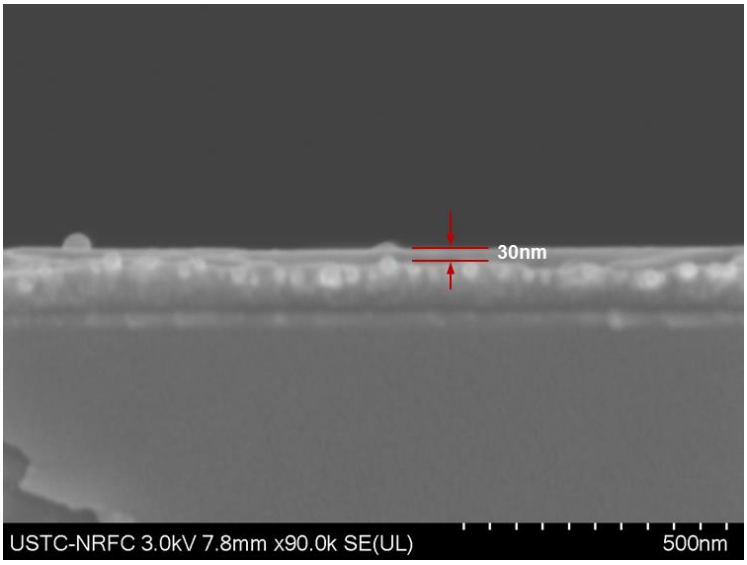

Figure S8. SEM images of emissive layer in the twisted-stacking hybrid film.

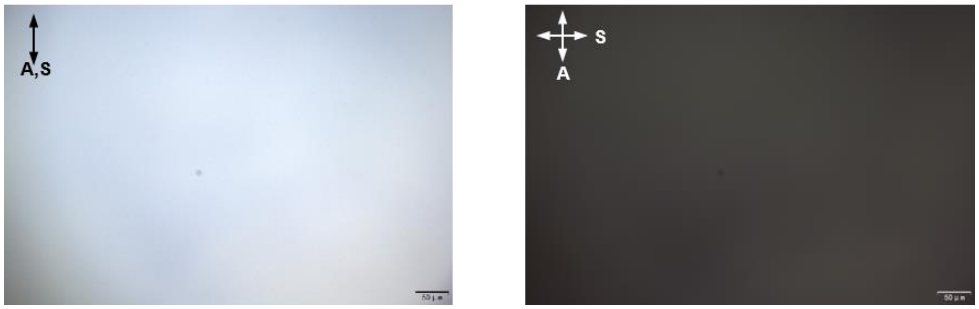

Figure S9. POM images of the emissive layer in the twisted-stacking hybrid film. The polarization direction of polarizer is A (analyzer). The orientation direction of the hybrid film is S. Scale bars: 50μm.

4. Rubrene was identified as the forth component, however "rubenene" was proposed by the the large language models (Figure S12).

Reply:

We sincerely apologize for this typographical error regarding the material name. The correct substance is rubrene, whereas the incorrect term "rubenene" was a spelling error introduced during the drafting process. We have thoroughly checked the full manuscript, figures, and supporting information, and have corrected this spelling throughout the text. Additionally, we have cross-checked all chemical terminology to eliminate similar errors and ensure the writing accuracy of the revised paper.

We have revised the Figure S12 in the supplementary information as Figure S15.

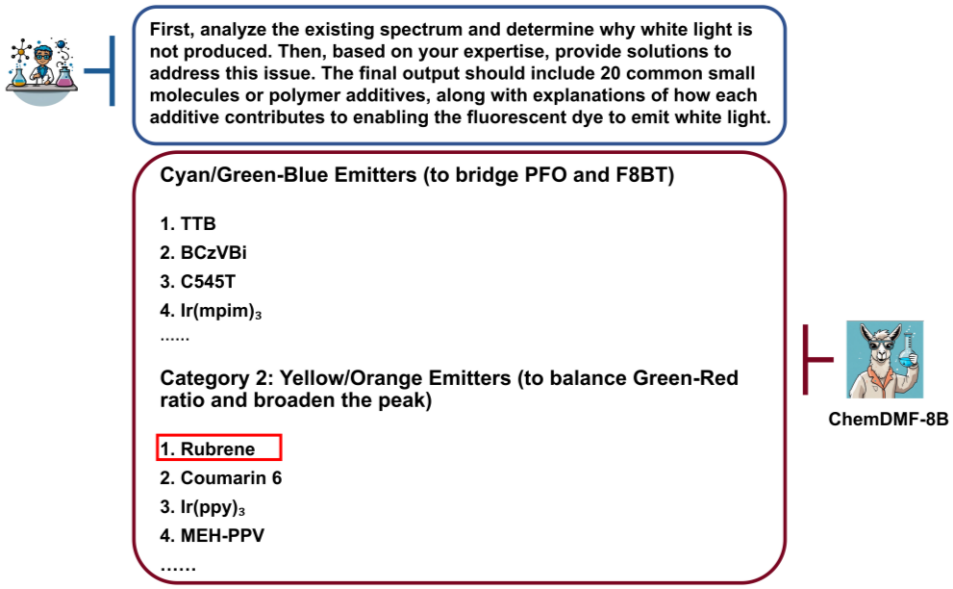

Figure S15. Schematic diagram of fluorescent molecules recommended by the large language models.

5. In Figure S7, dark lines are almost chromatically indistinguishable (40/80 μm, 50/100% and PFO/PFO-DBT). In part C, how is it possible that the PFO g_{lum} has a bisignate curve (~450/600nm) if the relative (monosignate) CPL maximum is located at ~430nm (Fig S9C,https://onlinelibrary.wiley.com/action/downloadSupplement?doi=10.1002/cjoc.70329&file=cjoc202501149-sup-0001-supinfo.pdf) ?

Reply:

We greatly appreciate the reviewer for the careful observation and valuable comments. To improve the visual resolution, we have re-adjusted the line color and gray scale of all curves and optimized the legend display contrast according to the reviewer's helpful suggestion, as shown in revised Figure S7. The revised figure has been updated in the **Supporting Information**.

To address the reviewer's concern regarding the different CPL profiles in Figures S7C and S9C, we clarify that this variation is intrinsic to the respective film designs

rather than an experimental inconsistency. The bisignate features centered at ~450/600 nm (Figure S7C) result from coupling the anisotropic fluorescent film with an overlying stretched PVA phase retarder. Conversely, the monosignate emission at ~430 nm (Figure S9C) originates from the twist-stacked configuration of two highly oriented PFO layers. These disparate configurations fundamentally alter the chiroptical pathways, leading to distinct CPL signatures and the observed spectral redshift.

We have revised the Figure S7 in the supplementary information as Figure S10.

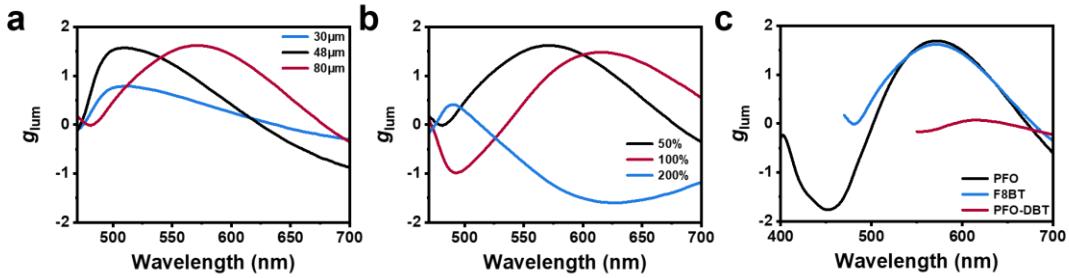

Figure S10. The variation of CPL spectra of chiroptical films with different parameters. The spectral lines of g_{lum} versus wavelength for heterostructure bilayer chiroptical films with different (a) thickness and (b) stretching degree of PVA layer, and (c) molecular selection of the highly oriented emissive layer.

Reviewer 2:

Comments to the Author

The manuscript proposes a novel dual-loop active learning framework that integrates a large language model (ChemDFM), a Wasserstein autoencoder (WAE), Gaussian mixture model-Markov chain Monte Carlo (GMM-MCMC) sampling, TabPFN regression, and Bayesian optimization to accelerate the discovery of high-performance white circularly polarized luminescence (WCPL) materials. Starting from the PFO/F8BT/PFO-DBT ternary system, the authors optimize the color rendering index (CRI) and CIE coordinates in Loop I, and the asymmetry factor (g_{lum}) and spectral fill factor (*FF*) in Loop II. Through iterative optimization, a quaternary system incorporating a fourth component (Rub) achieves outstanding performance: CRI > 90, CIE (0.33, 0.33), $|g_{lum}| \approx 1.8$, and $FF \approx 0.8$. Circularly polarized white organic light-emitting diodes (CP-WOLEDs) are successfully fabricated, demonstrating the ability to tailor the correlated color temperature (CCT) on demand. Overall, this work is innovative and has potential research impact, but the following aspects require revision and supplementation.

1. The formula (3) in the main text defines M = $|g_{lum}|$ × (Ra / 100), and it is reported that "our proposed hybrid films exhibit both high $|g_{lum}|$ of 1.8 and Ra of 90, leading to an exceptionally high M value up to about 1.62". However, in SI Table S1, the same set of data is given as $|g_{lum}|$=1.77, Ra=90, and M=0.89, which deviates from the main text by a factor of two. Moreover, the M values in the table do not appear to be calculated according to the formula in the main text. Please unify the definition of M between the main text and the SI, recalculate all comparative data, and revise Figure 3e and Table S1 if necessary.

Reply:

We highly appreciate the reviewer's meticulous review and valuable correction regarding the comprehensive parameter M. We sincerely apologize for the numerical discrepancies between the main text and Supporting Information, which resulted from an inadvertent calculation error during manuscript preparation.

In the revised manuscript, we have unified the calculation of M across all sections, figures, and tables, strictly adhering to the formula $M = |g_{lum}| \times (Ra/100)$. Accordingly, all entries in Table S1 and Figure 3e have been systematically recalculated and updated. For example, for the representative sample $|g_{lum}|$=1.8, Ra=90, the correctly calculated M value is 1.62, which now resolves the previous error (0.89) and perfectly aligns with the text.

These corrections ensure full data consistency between the main text and Supporting Information. We thank the reviewer again for helping us improve the precision and logical rigor of our manuscript.

The revised Table S1 is shown below:

Table S1. A comparison of the $|g_{lum}|$ and M values of representative WCPL materials and complexes documented in the literature and this study**.**

Category	g_{lum}	***Ra***	***M***	***Ref***
Chiral organic-inorganic hybrid	8×10^{-3}	93.4	7.5×10^{-3}	*1*
	1.56×10^{-2}	96.9	1.5×10^{-2}	*2*
	0.01	91	9.1×10^{-3}	*3*
	1.64×10^{-2}	81.2	1.3×10^{-2}	*4*
Chiral polymer	6.2×10^{-2}	98	6.1×10^{-2}	*5*
	1.4×10^{-2}	89	1.2×10^{-2}	*6*
	2.19×10^{-2}	97	2.1×10^{-2}	*7*
	1.8	90	1.62	***This work***
Chiral liquid crystals	1.88	82	1.5	*8*
	1	83	0.83	*9*
	0.46	94	0.43	*10*
Chiral inorganic	1.8×10^{-3}	81	1.5×10^{-3}	*11*
	0.01	88	8.8×10^{-3}	*12*
	2.32×10^{-2}	78	1.8×10^{-2}	*13*
	5×10^{-4}	89	4.5×10^{-4}	*14*
Chiral organic molecules	5×10^{-3}	60	3×10^{-3}	*15*
	3×10^{-3}	73	2.2×10^{-3}	*16*

2. In this work, an organic system with a g_{lum} as high as 1.8 was achieved, and the authors attribute this high g_{lum} to the optimized twisted-stacking structure. However, several control experiments may still be lacking, such as: (i) the g_{lum} of the emissive layer alone (without the PVA layer), (ii) the g_{lum} of the emissive layer combined with an unstretched PVA layer, and (iii) the g_{lum} of the emissive layer combined with a stretched PVA layer but with a twist angle of 0°. Without these baseline data, it is impossible to distinguish whether the high g_{lum} originates from the intrinsic chirality of the material, the linear polarization effect of PVA, or genuine circular polarization amplification arising from the twisted stacking. Therefore, it is recommended that at least above three types of control experiments be performed to improve the discussion of the high g_{lum} in this work.

Reply:

We sincerely appreciate the reviewer's constructive suggestions. We fully agree such systematic control measurements are indispensable to distinguish the contributions from intrinsic material chirality, linear polarization effects, and the twisted-stacking architecture to the giant g_{lum} value. According to the reviewer's advice, we have evaluated three recommended control configurations: (i) the isolated emissive layer, (ii) the emissive layer coupled with an isotropic PVA film, and (iii) the emissive layer with a stretched PVA film aligned at a 0° twist angle.

The results reveal that negligible CPL signals were detected in case (i) and (ii), ruling out intrinsic molecular chirality and confirming the inability of isotropic PVA layer to induce CPL. The fact that no CPL emission was induced at a 0° twist angle whereas a 45° configuration yielded CPL with a high g_{lum}, clearly demonstrates that polarization conversion is highly dependent on the twisted-stacking angle, which is consistent with previous work (Adv. Optical Mater. 2024, 12, 2301308). These control data clearly validate that the exceptional chiroptical performance originates predominantly from the twisted-stacking architecture rather than intrinsic chirality or trivial linear polarization effects.

We have added these control datasets and corresponding analyses "To elucidate the mechanism underlying the high g_{lum} achieved in the twisted-stacking composite films, three control configurations were evaluated. As shown in Supplementary Fig. 19, the pristine emissive layer alone (without PVA) demonstrated a negligible CPL response, confirming the inexistence of intrinsic molecular chirality. Furthermore, the emissive layer coupled with an unstretched (isotropic) PVA film exhibited no discernible chiroptical activity, indicating that isotropic PVA cannot induce CPL. In addition, aligning the stretched PVA with the emissive layer at a 0° twist angle yielded exclusively linear polarization features, failing to generate any effective CPL signals. Conversely, introducing a certain twist angle (twist angle $\neq 0^\circ$) enables the generation of CPL, with the polarization conversion reaching its maximum asymmetry factor at a twist angle of 45° to yield a giant g_{lum} up to 1.8. These control datasets clearly validate that the superior chiroptical performance is a direct consequence of the twisted-stacking architecture rather than intrinsic chirality or trivial linear polarization effects." into the revised manuscript (Page 9, paragraph 2) and **Supporting Information** according to the reviewer's helpful suggestions to enhance the scientific rigor and

persuasiveness of this work.

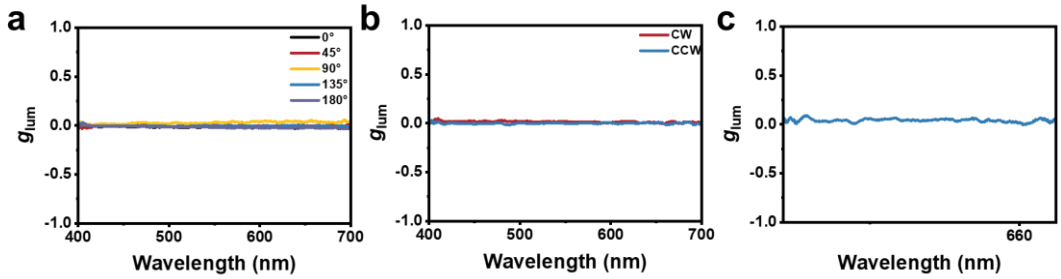

Figure S19. The variation of CPL spectra of chiroptical films with different parameters. The g_{lum} value of (a) the emissive layer alone, (b) the emissive layer combined with an unstretched (isotropic) PVA layer and (c) the emissive layer combined with a stretched PVA layer but at a twist angle of 0°.

3. The specific numerical values of the 147 ternary data points and 26 Bayesian optimization samples used for training the model (including composition ratios, spectra, CRI, CIE coordinates, g_{lum}, *FF*, thickness, stretch ratio, etc.) are not provided in a table or data file format; they are only schematically shown in SI Figure S5. According to the journal's data availability policy, key data supporting the conclusions should be made publicly available or at least provided as supplementary material. Please compile all training and validation data into an Excel/CSV file and upload it as SI, or provide a link to a public data repository.

Reply:

We sincerely appreciate the reviewer's careful attention to the journal's data availability policy. We fully acknowledge that providing the complete machine learning dataset in a standardized, reusable format is essential for transparency and reproducibility.

In response, we have compiled full training and validation dataset, comprising 239 data points and 26 Bayesian optimization samples. This compiled dataset explicitly details composition ratios, spectral data, CRI, CIE coordinates, g_{lum}, *FF*, film thickness, stretching degree, and other key parameters used for model training and validation. To ensure fully open access, this dataset has been deposited into a public, permanent, and citable data repository.

We have updated the **Data Availability** section (page 19, paragraph 2) in the revised manuscript to ensure full transparency, as shown below:

"Source data are provided with this paper. And the data are also available at https://doi.org/10.5281/zenodo.21132522. "

4. In the Dual-loop active learning strategy design, the authors state that "the resulting WCPL performance is returned to Loop I as an additional constraint, guiding the next compositional search." However, it is not specified in what form this return takes, whether the g_{lum} or *FF* is incorporated as part of the objective function to retrain the model in Loop I, or used as a screening threshold. The description in the text leans more toward a sequential execution: first, Loop I identifies the optimal composition, and then Loop II optimizes the structure for that fixed composition. Please provide additional details on the interaction mechanism of the dual loops to help readers understand how the two loops interact and form a closed loop.

Reply:

We thank the reviewer for pointing out that the interaction mechanism between the two loops was insufficiently clarified. We agree that the original description could give the impression of a purely sequential workflow. In the revised manuscript, we clarify that the dual-loop framework operates as a hierarchical closed-loop optimization process, where Loop II provides a feedback constraint to guide subsequent compositional exploration in Loop I.

More specifically, the interaction between the two loops does not occur through directly incorporating g_{lum} or *FF* into the Loop I objective function. Instead, the feedback is implemented as a feasibility-aware filtering mechanism.

In each iteration:

a) Loop I first screens and generates multiple candidate material compositions by active learning, which are optimized targeting white-light emission performances including CRI and CIE coordinates with the defined G score function.
b) All qualified candidate compositions from Loop I are forwarded to Loop II. Under the fixed composition, Loop II performs Bayesian optimization on twisted-stack processing parameters to maximize the WCPL comprehensive metric Q, as well as g_{lum} and spectral fill factor *FF*.
c) After structural optimization in Loop II, only those compositions that simultaneously possess excellent white-light quality (high G value) and satisfactory WCPL achievable performance (high Q value) are retained. These qualified composition–structure–performance paired data are augmented into the shared training dataset, which is used to retrain the WAE, GMM–MCMC and TabPFN models in Loop I for the next round of compositional iteration.

Instead, the experimentally obtained WCPL performance from Loop II is fed back to ChemDFM, which serves as the decision-making module for proposing the next-round compositions. Therefore, Loop II effectively acts as a downstream physical-performance constraint on Loop I.

We have revised the manuscript to explicitly clarify this interaction mechanism in Section "Dual-loop active learning strategy design".

" The two loops operate in a coupled hierarchical manner rather than as fully independent sequential modules. Loop I proposes candidate compositions optimized for white-light emission properties (CRI and CIE coordinates), which are subsequently

evaluated in Loop II through structural optimization of the twisted-stack architecture. The resulting WCPL performance metrics (g_{lum} and *FF*) are not directly incorporated into the Loop I regression objective; instead, they serve as experimentally validated feasibility constraints. Only compositions that simultaneously exhibit favorable white-light emission and acceptable WCPL performance after Loop II optimization are retained and added back into the active-learning dataset. The output of Loop II is not used simply as an optimized processing condition, nor does it directly replace the objective function of the Loop I prediction model. Instead, the experimentally optimized WCPL performance is returned to ChemDFM as feedback. ChemDFM then integrates the Loop I prediction results, the Loop II experimental outcomes, and accumulated chemical knowledge to recommend new compositions for the next Loop I cycle."

5. In the Iterative optimization of WCPL based on the ternary systems, it is stated that "The search space was bounded to 20 μm ⩽ thickness ⩽ 80 μm and 10% ⩽ stretching degree ⩽ 150%." This implies that thickness is treated as a continuous interval between 20 and 80 μm for running Gaussian process regression and acquisition function optimization. However, the Methods section shows that the actual available PVA film thicknesses are only three discrete values: 30 μm, 48 μm, and 80 μm, which introduces some ambiguity. It is necessary to clarify whether, if the optimization algorithm recommends a value such as 30.8 μm, the closest experimental thickness is chosen around the recommended value. Alternatively, the search space for Bayesian optimization should be redefined as the discrete set {30, 48, 80}, with the kernel function adjusted accordingly. If the authors actually achieved intermediate thicknesses by stacking multiple layers or multi-step stretching, this should also be explicitly stated.

Reply:

We greatly appreciate the reviewer for pointing out this ambiguous description regarding the search space and experimental constraints of PVA film thickness.

As the reviewer correctly deduced, while the Bayesian optimization algorithm operated across a continuous interval (20–80 μm) for modeling purposes, our practical experiments were restricted by commercial availability to three discrete thicknesses: 30 μm, 48 μm, and 80 μm. Therefore, whenever the algorithm recommended an intermediate continuous value (such as 30.8 μm), we simply selected the nearest available discrete thickness for actual sample fabrication and experimental validation.

We have added a detailed explanation in the **Methods** section to elaborate on the discrete thickness constraints and the above screening principle, as shown below:

"Restricted by practical experimental conditions and commercial specifications, only three discrete PVA thicknesses (30 μm, 48 μm, and 80 μm) were available,and the stretching degree was controlled within the range of 10 ~150%. During Bayesian optimization, the algorithm predicted continuous thickness values within the defined range, and the nearest available discrete thickness was selected for experimental validation in each iteration."

Reviewer 3:

Comments to the Author

This manuscript reports an active learning including Bayesian optimization guided strategy for optimizing material compositions and processing parameters to obtain high-performance white circularly polarized films, and demonstrates a closed loop from model prediction to experimental validation. The topic is timely, and the overall workflow is potentially valuable for data-driven materials optimization. However, several important issues remain insufficiently addressed.

1. Please provide more justification for the use of a WAE latent space in Loop I. Considering ternary or quaternary compositional systems, the intrinsic dimensionality remains limited under simplex constraints, and it is therefore not yet clear that latent space modeling is necessary. The authors should clarify the advantage WAE provides over operating directly in the original composition space.

Reply:

We thank the reviewer for this insightful comment. We agree that the compositional space of ternary or quaternary systems is intrinsically low-dimensional under simplex constraints. However, the key motivation for introducing the WAE is not dimensionality reduction per se, but rather to learn a structure-aware and distribution-regularized representation of the composition–property landscape, which enables efficient generative exploration.

Specifically, although the composition lies in a simplex, the corresponding optical performance (e.g., CRI and CIE coordinates) is governed by highly nonlinear interactions such as Förster resonance energy transfer (FRET), which distort the effective structure–property relationship. As a result, high-performing regions are not uniformly distributed nor easily separable in the original compositional space.

The WAE provides two critical advantages:

a) Nonlinear manifold learning of performance-relevant structure

The latent space organizes compositions according to their optical performance, forming distinct clusters ("islands") of high and low performance, as observed in Fig. 2a. This structure is not explicitly visible in the original simplex representation.

b) Enabling distribution-aware generative sampling

By mapping the constrained simplex to a smooth latent space, the WAE allows efficient modeling using GMM and sampling via MCMC. This is difficult to implement directly in the simplex due to boundary constraints and non-Gaussian distributions.

Therefore, the WAE serves as a reparameterization of the compositional space aligned with the underlying performance distribution, enabling more efficient exploration than direct sampling in the original space.

We have revised the manuscript in Section "Dual-loop active learning strategy design": "Rather than serving purely as a dimensionality reduction tool, the Wasserstein Autoencoder (WAE) learns a smooth and physically meaningful latent representation that aligns the compositional space with the underlying performance landscape. Although the original composition lies on a low-dimensional simplex, the

corresponding structure–property relationship is highly nonlinear due to intermolecular interactions such as Förster resonance energy transfer (FRET). The WAE effectively "unfolds" this distorted space, organizing compositions with similar optical performance into contiguous regions in latent space, thereby facilitating efficient exploration and sampling. This reparameterization enables the use of Gaussian mixture modeling and MCMC sampling in a continuous and unconstrained latent space, which is difficult to achieve directly in the original simplex coordinates."

2. The proposed framework may be overengineered for the limited dataset (e.g. 272 samples for WAE and 26 for BO). Under such small data conditions, complex models may be unstable and difficult to validate rigorously. Therefore, stronger evidence is needed to justify the methodology, for example through learning curves, repeated cross-validation, etc.

Reply:

We appreciate the reviewer's concern regarding model complexity under limited data conditions. First, we emphasize that the proposed framework is specifically designed for small-data regimes typical of experimental materials discovery, and incorporates multiple mechanisms to ensure robustness and stability.

Second, the role of each model was chosen to match the corresponding data regime. The WAE in Loop I is used mainly as a regularized generative manifold-learning tool for candidate generation, rather than as the final property predictor. The final ranking of decoded candidates is performed by the TabPFN regressor, which was specifically developed for small tabular datasets and requires little task-specific training. For Loop II, Bayesian optimization is applied only to a two-dimensional processing space, namely PVA thickness and stretching degree, with the twist angle fixed at ±45°. Gaussian-process-based Bayesian optimization is particularly suitable for such low-dimensional and experimentally expensive optimization problems.

a) Active learning paradigm improves data efficiency

The model is not trained once on a fixed dataset; instead, it is iteratively updated with experimentally validated samples. This closed-loop design significantly improves sample efficiency and mitigates overfitting by continuously refining the model with high-value data.

b) Lightweight model design

The WAE employed in this work is a relatively small fully connected network (four-layer MLP with a 2D latent space), rather than a large deep model. This reduces the risk of overfitting and ensures stable training even with limited data.

c) Rigorous cross-validation and benchmarking

As described in the Methods section, we performed 5-fold shuffle-split cross-validation to evaluate multiple regression models. The selected model (TabPFN) achieves strong predictive performance ($R^2 = 0.88$) on unseen data, indicating good generalization

despite the small dataset.

d) Empirical evidence of stability and efficiency

The framework consistently improves target metrics within only a few iterations, demonstrating high sample efficiency and stable convergence.

3. The description of Loop II needs further clarification. The manuscript indicates that Bayesian optimization was performed with a GP surrogate, while several other regressors (including TabPFN) were benchmarked separately. The authors should clarify the role of these models and explain why GP, rather than the best-performing regressor, was used in the BO loop.

Reply: We thank the reviewer for pointing out the need for clarification. The apparent discrepancy arises because the regression models and the Gaussian Process (GP) serve different roles in our framework.

The regression models (including TabPFN, Random Forest, XGBoost, etc.) are used for predictive benchmarking and feasibility assessment of the underlying structure–property mapping. Their role is to evaluate whether the sparse discrete experimental observations can be reliably approximated by a smooth learnable response landscape suitable for surrogate-based optimization. In general, all regression models considered in this work, can learn a processing–property mapping from discrete experimental observations,

$$\mathcal{D}_n = \{(x_i, Q_i)\}_{i=1}^{n}$$

where x_i is the processing-parameter vector, for example,

$$x_i = \left[t_{PVA,i}, s_i\right],$$

with t_{PVA} representing the PVA thickness and s representing the stretching degree. Q_i is the target performance metric. The regression task can therefore be expressed as

$$Q = f(x),$$

and a trained regression model provides a point prediction at an untested processing condition x^*,

$$\hat{Q}(x^*) = \hat{f}(x^*).$$

In Loop II, however, the closed-loop Bayesian optimization was performed using a Gaussian-process surrogate. Bayesian optimization requires not only a prediction of the objective value but also a calibrated uncertainty estimate at each unexplored point. Therefore, BO does not simply select the next experiment by maximizing the predicted value,

$$x^* = \arg\max_{x \in \mathcal{X}} \hat{Q}(x).$$

The reason for using GP is that Bayesian optimization requires not only a prediction of the objective value but also a calibrated uncertainty estimate at each unexplored point. The GP naturally provides a posterior mean and posterior variance, which can be directly used to construct acquisition functions such as Expected Improvement and

Upper Confidence Bound. This is particularly suitable for our Loop II problem because the optimized processing space is low-dimensional, involving mainly PVA thickness and stretching degree, and each experimental evaluation is costly.

The choice of GP is motivated by the following considerations:

a) Uncertainty estimation for acquisition functions

Bayesian optimization relies on acquisition functions such as Expected Improvement (EI) and Upper Confidence Bound (UCB), which explicitly require both predictive mean and uncertainty (variance). GP provides well-calibrated uncertainty estimates, while models such as TabPFN do not natively provide reliable uncertainty estimates in this setting.

b) Stability in low-data regimes

GP models are known to perform robustly with small datasets, offering smooth function approximation and interpretable uncertainty, which is critical for guiding experimental exploration.

c) Compatibility with BO framework

The EI–UCB acquisition strategy used in this work directly depends on the posterior distribution provided by the GP. Replacing GP with other models would require additional uncertainty calibration, which is non-trivial and beyond the scope of this study.

TabPFN is used to validate that the structure–property mapping is learnable and to benchmark predictive performance, but is not directly used in BO due to its lack of explicit probabilistic outputs.

Therefore, GP is selected not because of superior predictive accuracy, but because of its suitability as a probabilistic surrogate for efficient and stable Bayesian optimization.

We have revised the manuscript in section **Methods**:

"The experimentally measured processing–property dataset was denoted as

$$\mathcal{D}_n = \{(x_i, Q_i)\}_{i=1}^{n},$$

where$x_i$is the processing-parameter vector and Q_i is the target metric. In this work,

$$x_i = [t_{PVA,i}, s_i],$$

where t_{PVA} and s represent the PVA thickness and stretching degree, respectively. The regression task can be written as

$$Q = f(x),$$

where $f(x)$ is the unknown processing–property response function. A trained regression model can estimate the target value at an untested processing condition x^* as

$$\hat{Q}(x^*) = \hat{f}(x^*).$$

Thus, all regression models considered in this work, including GP, TabPFN, Random Forest, XGBoost, and CatBoost, can in principle learn a predictive response surface from discrete experimental observations."

4. A structure comprising a commercial UV LED chip externally coupled to emissive films is an optically photoluminescence-based color conversion device, not an OLED or CP-WOLED. The use of "electroluminescence" and "CP-WOLED" should be revised.

Reply:

We sincerely appreciate the reviewer's careful and professional comments on the expression of device structure and luminescence mechanism. As the reviewer pointed out, the device in this work consists of a commercial UV LED chip externally coupled with emissive films, which realizes color conversion through photoluminescence (PL) rather than electroluminescence. We fully agree that the descripyion of OLED or CP-WOLED is inappropriate. We have carefully revised the relevant descriptions in the manuscript according to the reviewer's suggestion. All inaccurate terms involving electroluminescence and CP-WOLED have been deleted or corrected to **white circularly polarized photoluminescent (WCP-PL) device** and other accurate expressions. Furthermore, we have reviewed and standardized the descriptions of the device's working principle and structural characteristics to ensure the scientific rigor.

5.The current data do not seem sufficient to justify stronger statements such as "direct deployment" in illumination or full-color 3D display applications. For a UV-LED-excited conversion device, application relevance should be supported by additional metrics such as photostability under continuous UV irradiation, operational lifetime, color stability over time, conversion efficiency or luminous efficacy, etc.

Reply:

We greatly appreciate the reviewer's critical and valuable comments on the application-oriented performance and practical potential of our UV-LED-excited photoluminescence conversion films. We fully agree that the statement of direct deployment in practical illumination and full-color 3D display is overstated, and the current data are insufficient to fully support such practical application claims.

In response to this concern, we have revised the overestimated descriptions throughout the manuscript. Terms like "direct deployment" has been replaced with more scientifically accurate and conservative expressions, such as "promising potential". Furthermore, we have supplemented comprehensive application-relevant characterizations, including UV photostability, time-dependent color stability, and external quantum efficiency (EQE) to substantiate the practical relevance of our work. These new datasets significantly bolster our revised conclusions.

We have updated the manuscript and Supporting Information accordingly, with the following text added to the main discussion (Page 10, paragraph 3), as shown below:

"We further conducted a series of systematic device-targeted characterizations covering UV photostability, temporal color retention and external quantum efficiency (EQE). The resulting conversion film exhibited robust practical performance (Supplementary Fig. 20-22). Notably, the CPW-PL device retains a $|g_{lum}| > 1.2$ across the entire visible range (Fig. 4d), confirming its strong potential for future use in uniform-illumination

and full-color 3D display prototypes."

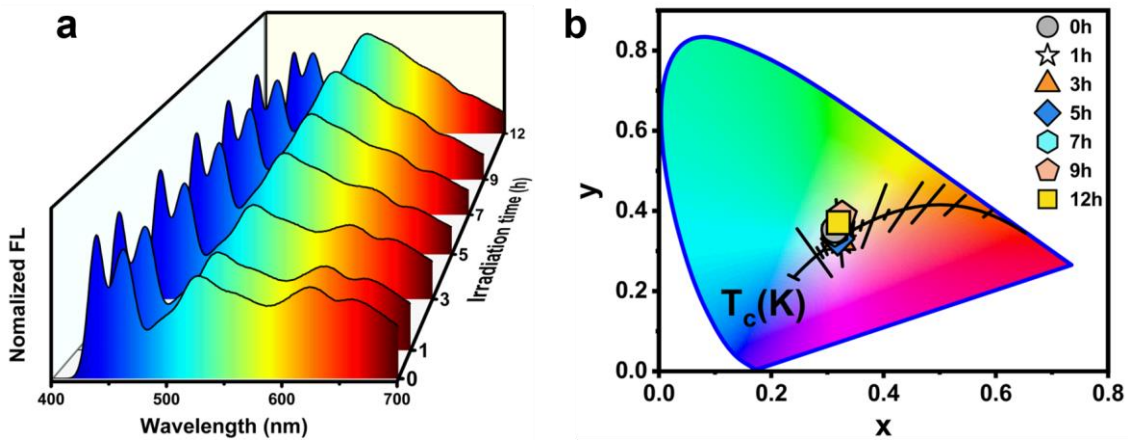

Figure 20. Long-term UV irradiation photostability of the WCPL conversion film under continuous UV-LED excitation for 12 h. Time-dependent evolution of (a) normalized FL emission intensity and (b) CIE 1931 chromaticity coordinates of the film recorded at irradiation durations of 0,1,3,5,7,9, and 12 h.

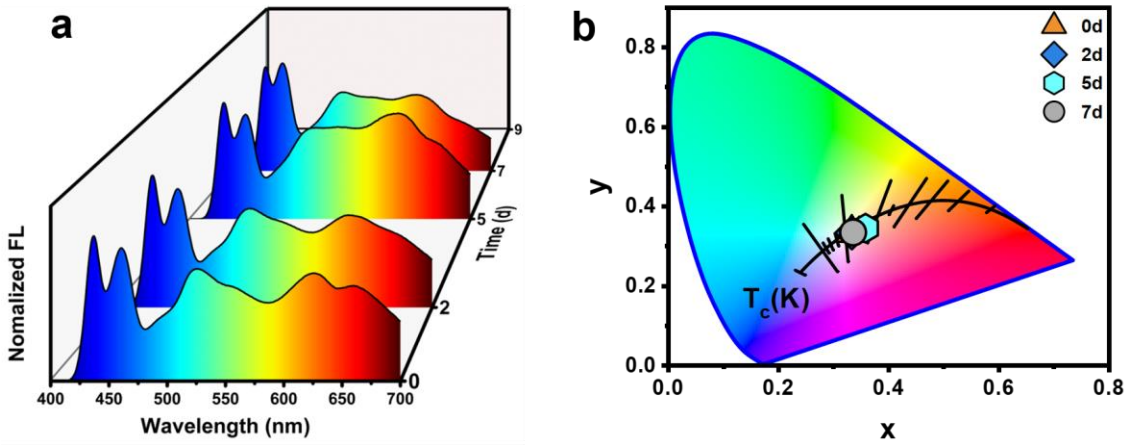

Figure S21. Environmental stability of the WCPL conversion film. (a) FL spectra and (b) CIE chromaticity coordinates of samples stored under ambient conditions at room temperature for different durations.

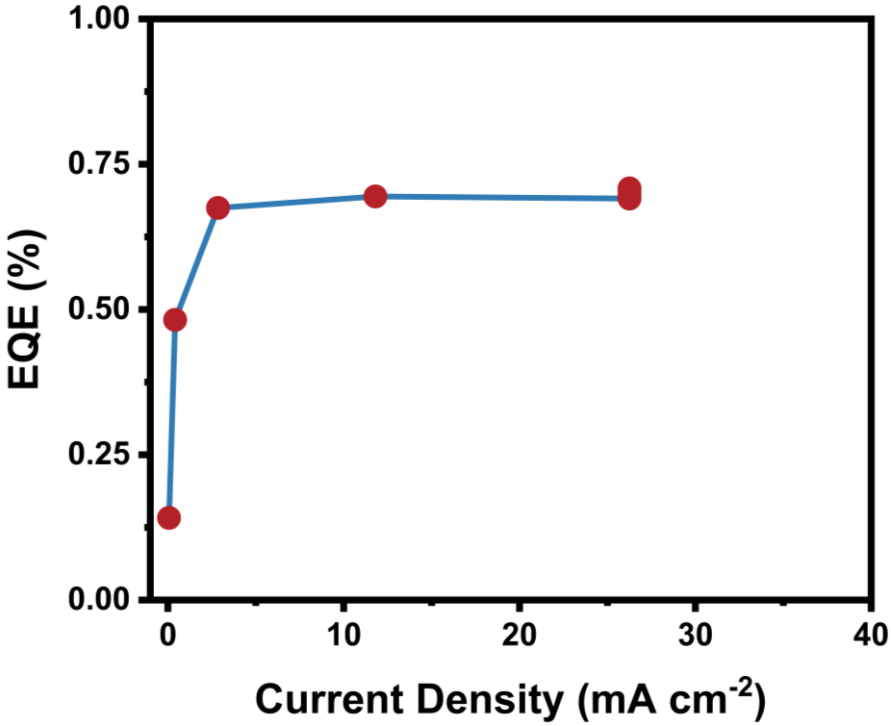

Figure S22. The performance of the CPW-PL device. EQE vs current density curves.

6.The conclusion may be somewhat overgeneralized. The present work demonstrates a promising proof-of-concept in a specific system, but the broader claim of "great fundamental value" for the accelerated discovery of novel optically functional materials and devices appears stronger than what is directly supported by the current results. A more cautious and specific conclusion would be more appropriate.

Reply:

We sincerely appreciate the reviewer's constructive comment on the generalization of our conclusion. We agree that the statement regarding "great fundamental value for the accelerated discovery and optimization of novel optically functional materials and devices" may be overgeneralized, given that the current methodology was demonstrated specifically within the CPW-PL film system. Accordingly, we have revised the conclusion and moderated the language to emphasize the proof-of-concept nature of our dual-loop machine learning strategy, specifically in the context of circularly polarized luminescent materials. The revised conclusion better reflects the actual contribution and the limitations of the current work, and we believe this adjustment significantly improves the accuracy and objectivity of the manuscript.

The revised conclusion have been incorporated into the revised manuscript (page 11, paragraph 4), as shown below:

"In summary, we proposed a dual-loop machine learning strategy that integrates active learning with LLMs, which enables the efficient identification of both compositional and processing parameters for a predefined set of target properties. Multi-objective optimization of WCPL performance is thus achieved with limited experimental runs.

This strategy enables the precise fabrication of WCPL films with an excellent CRI of 90 at the ideal CIE coordinates of (0.33, 0.33) and a uniformly high g_{lum} (up to 1.8) across the full visible spectrum. To summarize, the on-demand manufacturing of WCP-PL device with excellent CRI at the ideal CIE coordinates, a high g_{lum} value as well as a customized CCT is realized, thus facilitating their practical application in lighting and full-color 3D display. Furthermore, our results provide a promising proof-of-concept strategy for the accelerated optimization of circularly polarized luminescent materials, demonstrating the potential of integrating active learning with LLMs in materials science."

7.The current data availability statement is inadequate for a data-driven study, as the dataset is central to the main claims and necessary for reproducibility. The authors should publicly release the data required to reproduce the main results, or clearly justify any restrictions.

Reply:

We sincerely appreciate the reviewer's valuable comment on the data availability statement. We fully agree that for a data-driven study, providing open access to the training and validation datasets is essential for ensuring reproducibility and rigorous scientific validation. In response, we have compiled the complete dataset, including the experimental measurements, processing parameters, and machine learning inputs into a standardized format. This dataset has been deposited into a permanent public repository.

We have updated the **Data Availability** section (page 19, paragraph 2) in the revised manuscript to ensure full transparency, as shown below:

"Source data are provided with this paper. And the data are also available at https://doi.org/10.5281/zenodo.21132522."

8.The claimed superiority over literature is not fully convincing without comparable measurement conditions, especially since CPL-related metrics such as g values are highly sensitive to calibration and testing procedures. Stronger validation of the key metrics is therefore needed, including reproducibility, uncertainty estimates, and preferably independent verification.

Reply:

We sincerely appreciate the reviewer's highly constructive comment on the validation of CPL-related key metrics. We fully agree that g_{lum} values are sensitive to instrument calibration, optical geometry, and measurement procedures, which usually leads to variations in reported values across different experimental setupsand. To address the concern regarding data reliability, we have standardized measurement conditions. The CPL measurement protocols, including specific instrument settings, excitation wavelengths, and scanning parameters maintained consistency across all test.

Moreover, we have performed measurements on independently prepared samples

to verify the consistency of our results. These control tests demonstrate that while minor variations,the signal stayed largely consistent.

Thus, we have clearly specified complete and standardized CPL test conditions in the revised **Methods** as "Circularly polarized luminescence (CPL) spectra were recorded on a Jasco CPL-300 spectrofluoropolarimeter under standardized conditions: excitation wavelength λex = 365 nm, D.I.T. = 0.5 sec, Measure range=700 - 400 nm and Scanning speed = 1000 nm/min."

In addition, We have revised the literature comparison statements to avoid overclaiming superiority although all comparisons are contextualized within our standardized measurement parameters. The revised objective and rigorous descriptions were added to the manuscript (page 10, paragraph 2) as follows: "In contrast, our twist-stacking architecture enables simultaneous strong chiroptical activity and high color quality, yielding highly competitive WCPL characteristics under our standardized measurement conditions."

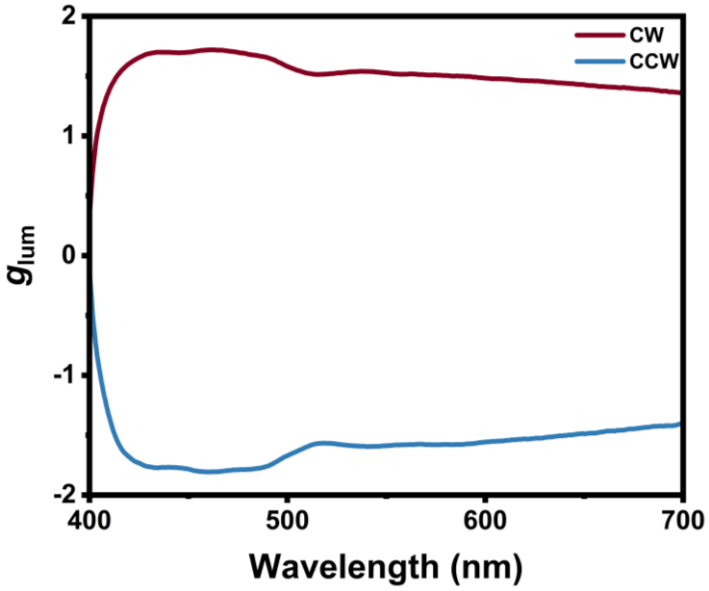

Figure. CPL spectra of the independently re-prepared optimal sample from the quaternary system with twisted-stacking structures.

中国科学技术大学
University of Science and Technology of China

Prof. Gang Zou
Department of Polymer Science and Engineering
University of Science and Technology of China
Jinzhai Road 96#, Baohe District, Hefei 230026 China
Email: gangzou@ustc.edu.cn

August 16, 2026

Dear Editor，

Thank you very much for your e-mail dated on 3- August -2026 regarding the revision on the above manuscript (NCOMMS-26-027357). On behalf of all the authors, I would like to express our sincere gratitude to you and the reviewers for your careful consideration of our manuscript titled "Design of White Circularly Polarized Luminescence with High g_{lum} Across Entire Visible Regions by Dual-Loop Active Learning" submitted to your esteemed journal. Based on the reviewers' comments, we have meticulously revised our manuscript. The details of the point-by-point response are given on the 2nd page. The editorial requests have been addressed according to the attached Author Checklist.

In accordance with your key suggestion, we have added a targeted discussion in the second paragraph of the Introduction section to compare our work with the reported study (https://doi.org/10.1002/cjoc.70329). "Recently, we exploited a twisted-stacking architecture to achieve multi-modal information encryption[15]. This structure is constructed by overlaying highly oriented achiral polyfluorene micropatterns onto uniaxially stretched PVA retardation layers, which delivers strong chiroptical activity. In principle, this system can produce CPL with arbitrary desired spectroscopic features, WCPL for instance, provided that an appropriate combination of formulation and processing parameters is identified."

The current manuscript proposes a dual-loop active learning strategy to tackle the combinatorial bottleneck for WCPL generation. Our previous work, which relied on a comparable material system, realized multi-modal information encryption through conventional AI-free forward design approaches. By contrast, the present work leverages a data driven dual-loop workflow to efficiently explore the high dimensional parameter space and bypass the prohibitive cost of exhaustive experimental screening.

We hope the present manuscript have been promoted greatly and now it could satisfy the quality required by your esteemed journal. Thank you very much again for your efforts in this regard, and we look forward to hearing from you soon.

Sincerely

Gang Zou

Reviewer 1:
Comments to the Author

The authors of the present manuscript (NCOMMS-26-027357A) took a good wealth of time to respond to the reviewers' comments and questions, explaining their point of view in good detail in the responses to the reviewers and transferring a few of the explained changes in the text (and SI). In my opinion, points 2-5 were carefully addressed, but point 1 (the key-one) is not clarified yet.
At this point, I would like to make some more comments: considering a chronological timeline, authors affirmed that "The published article (https://doi.org/10.1002/cjoc.70329) was a subsequent empirical validation inspired by the preliminary material screening of this overarching project" and that "the material systems adopted in both studies were initially screened and recommended by ChemDFM, an in-house, chemistry-oriented large language model proposed in this work", but in the published article authors wrote that a biomimetic approach (mentioning also the Chrysina gloriosa) was adopted and no chemistry-oriented large language model (ChemDFM) was cited in their biomimetic design strategy for polyfluorenes selection. How is it possible? Again, if the published articles was an experimental characterization and performance validation, why did not authors cite it in the bibliography of the current submitted manuscript? The published article was accepted on 25 September 2025 (much earlier than the present submission). Coherently with my first revision, I still think that the present article has a remarkable conceptual overlap with the published work, even if some novelties (already discussed) were introduced. As stated by the authors "The present work achieves a systematic optimization of compositional and processing parameters ". At this point, I think that editor should decide if an AI-driven implementation for a forth component (rubrene) and a WCPL device prototype are a valid advancement (compared to the published article) which deserves a publication on Nature Communication.

Reply:
We sincerely thank the reviewer for the thorough, rigorous follow-up comments concerning the logical consistency, citation omission and conceptual overlap between our manuscript and the published article (DOI: 10.1002/cjoc.70329). We address each of your questions point-by-point as follows,

1. These two studies differ markedly in scope, complexity, and novelty. The prior work achieved single-band circularly polarized luminescence from single-component emitters under fixed experimental conditions without adopting other AI tools, with its research scope covering biomimetic fabrication, multicolor CPL amplification, programmable micropatterns, Janus displays, and information encryption. By contrast, the present manuscript addresses a distinct optimization problem: identifying formulation-process combinations within a limited experimental budget that simultaneously satisfy white chromaticity, high CRI, large g_{lum} , and broad CPL spectral coverage. Accordingly, the key contributions of this work reside in the closed-loop, dual-stage multi-objective optimization strategy implemented for

multicomponent WCPL systems, together with user-defined CCT targets and device-level experimental validation.

2. The project timeline is elaborated as follows. The present research was initiated in August 2024, during which the initial ChemDFM-driven database for three-component material screening was constructed to serve as the research foundation. In January 2025, a new group member, Baiheti (first author of the *Chinese Journal of Chemistry* article, DOI: 10.1002/cjoc.70329), launched a side project based on our pre-established experimental platform. The experimental design was straightforward and did not require sophisticated optimization. That side-project manuscript was submitted on 25 August 2025, rapidly accepted on 25 September 2025, and published online on 23 October 2025. No AI tools were employed in that work, apart from preliminary candidate selection suggested by consulting an LLM; this minor detail was not documented in the original publication. By comparison, the main project, presented in this manuscript, led by Yang, targets high-performance white circularly polarized luminescence, simultaneously achieving high g_{lum} (>1) and *FF* (>0.5), and an excellent CRI value (>85) at the ideal CIE coordinates (0.33,0.33). It demands multi-objective optimization within a high-dimensional parameter space, iterative ChemDFM-assisted material screening, and fabrication of functional WCPL devices. The substantial computational and experimental workload explains its later submission.
3. The omission of the CJC paper in our originally submitted manuscript was an inadvertent oversight. We have now supplemented the full citation for this work and incorporated brief relevant discussions in the Introduction section (Page 2, Paragraph 2).

We appreciate the reviewer for pressing us to correct the chronology and to state the overlap transparently. These revisions substantially narrow and clarify the novelty claim.

Reviewer 2:

Comments to the Author

The authors have answered all questions, and I suggest to accept in present version.

Reply:
We sincerely appreciate your thorough evaluation, positive affirmation, and valuable recommendation for the acceptance of our manuscript. We are deeply grateful for your professional guidance throughout the revision process, which has significantly polished and improved the quality of our work. We confirm that all revisions have been fully completed and integrated into the final version of the manuscript. Thank you again for your time and efforts in reviewing our paper.

Reviewer 3:

Comments to the Author

The authors have addressed the concerns I previously raised, and I am pleased to see a significant improvement in the scientific rigor and overall quality of the paper. I do not have any further questions or issues to raise.

Reply:
We greatly appreciate your positive evaluation and constructive comments, which have helped us substantially improve the scientific rigor and quality of this manuscript. We have carefully revised the manuscript according to all suggestions. Thank you again for your time and efforts.